108. Two-State Reactivity in Organometallic Gas-Phase Ion Chemistry

by **Sason Shaik**[a])*, **David Danovich**[a]), **Andreas Fiedler**[b]), **Detlef Schröder**[b]), and **Helmut Schwarz**[b])*

[a]) Department of Organic Chemistry and the Fritz Haber Center of Molecular Dynamics, The Hebrew University, Jerusalem 91904, Israel

[b]) Institut für Organische Chemie der Technischen Universität Berlin, Strasse des 17. Juni 135, D–10623 Berlin

Dedicated to *Sir Derek H. R. Barton*

(21.VII.95)

In contrast to organic reactions, which can almost always be described in terms of a single multiplicity, in organometallic systems, quite often more than one state may be involved. The phenomenon of two states of different multiplicities that determine the minimum-energy pathway of a reaction is classified as two-state reactivity (TSR). As an example, the ion/molecule reactions of 'bare' transition-metal-monoxide cations with dihydrogen and hydrocarbons have been analyzed in terms of the corresponding potential-energy hypersurfaces. It turns out that, besides classical factors, such as the barrier heights, the spin-orbit coupling factor is essential, since curve crossing between the high- and low-spin states constitutes a distinct mechanistic step along the reaction coordinates. Thus, TSR may evolve as a new paradigm for describing the chemistry of coordinatively unsaturated transition-metal complexes. This concept may contribute to the understanding of organometallic chemistry in general and for the development of oxidation catalysts in particular.

Introduction. – The role of concepts which can provide new insight in chemical problems can hardly be overemphasized, and the present article describes the *two-state-reactivity* (TSR) paradigm and its manifestation in H–H and C–H bond activation by 'bare' oxo-cations MO^+ of the late, first-row transition metals Mn–Cu [1] [2].

With a few notable exceptions, for example O_2 and CH_2, organic species generally possess low-spin ground states, and their reactions proceed on a single potential energy surface; this will be referred to as *single-state reactivity* (SSR). To conceptualize the key features of SSR, it is in principle sufficient to understand the transition structures (TSs), their entropic requirements, and the associated barrier heights. Indeed, the arsenal of reactivity paradigms that has evolved in organic chemistry, such as linear free energy relationships [3], frontier molecular orbital theory [4], the *Woodward-Hoffmann* rules [5], and the valence bond (VB) crossing diagrams [6], all are related to SSR. Thus, our intuition derives from the experience with surfaces of a single multiplicity. In fact, even photochemical *reactivity* in the sense of cleavage and formation of chemical bonds is basically treated on a single (though excited) potential-energy hypersurface. Nevertheless, it is clear that SSR is only one aspect in chemical reactivity.

Coordinatively unsaturated transition-metal compounds often possess high-spin ground states and nearby low-spin excited states [7–9]. As a result of the adjacency of these spin states, the reactivity of these compounds may generally involve (at least) two states in which the ground state must not necessarily be the most reactive one. TSR is characterized by a crossing of two potential-energy hypersurfaces of different multiplic-

ities in which the crossing represents a distinct mechanistic step along the reaction coordinate. Therefore, entirely new reactivity factors evolve due to different bonding requirements in both states as well as due to the transition probabilities between the surfaces. It is the interplay of these TSR factors with the classical SSR features, such as transition structures and barrier heights, that makes TSR not only intriguing and challenging, but also of fundamental importance for organometallic chemistry.

Gas-phase ion chemistry provides a straightforward experimental and theoretical framework for the study of SSR and TSR due to the fact that there are no interfering effects of solvents, aggregation phenomena, counter ions *etc.* [2]. In 1994, *Armentrout* and coworkers [10] and we [1] [11] have independently encountered manifestations of TSR in the bond activation of dihydrogen and of simple alkanes by the 'bare' metal-oxide cations FeO^+ and CoO^+, reactions which represent a model for C–H bond activation and functionalization of alkanes [12].

In this article, we outline the key features of the TSR paradigm as compared to the classical SSR approach. First, we will address R–H bond activation by MO^+ cations (M = Cr–Cu), and the electronic structures of the metal oxides will be discussed. Then, the different features of SSR and TSR will be described for hydroxylations of R–H (R = H, alkyl) by MO^+, and components which influence reactivity in bond activation and product formation will be analyzed. Finally, the probability for spin-inversion processes in these reactions will be addressed together with ways how to circumvent the spin-inversion bottleneck.

R–H Bond Activation by MO^+: A Brief Description. – Here, we would like to give an overview of the features of gas-phase reactions of MO^+ cations with organic substrates [1] [2]. Due to the relevance of iron-oxenoids in catalysis and biochemistry [13], as well as the fact that most of the experimental studies deal with FeO^+, we will focus on iron. While reactivity studies have also been performed for other MO^+ cations, the gas-phase chemistry of CuO^+ has not been studied yet.

Scheme 1 illustrates the richness of the chemistry of FeO^+ with dihydrogen [10a] [11a], alkanes [14], benzene [15], toluene [16], and other arenes [17]. In the reaction with H_2, the products Fe^+ and H_2O are formed *via* an initial insertion (*I*) process which is extremely

Scheme 1

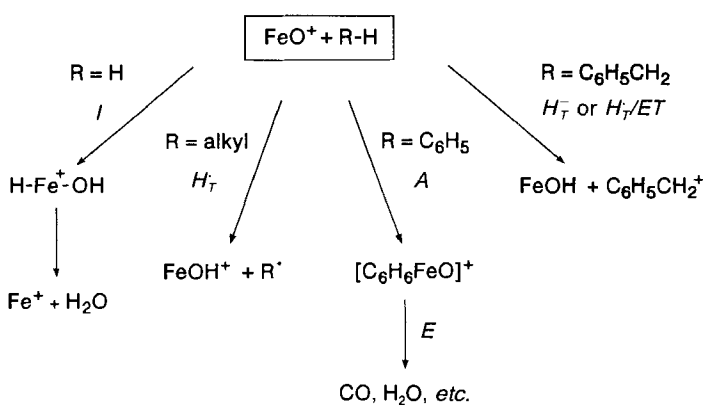

inefficient and occurs only once in every 100–1000 collisions[1]). In contrast, the reactions with alkanes [14] are more efficient and appear to commence with H-atom transfer ($H_T^{\cdot}$). While CoO^+ and NiO^+ behave quite similar to FeO^+ [10b] [11], the MnO^+ cation [19] reacts efficiently with alkanes and also H_2 involving the *I* as well as the $H_T^{\cdot}$ channels.

Yet another mechanism is operative in the reactions of FeO^+ with ethene [20] and benzene [15a], and this can be classified as an addition-elimination (*AE*) type. Here, FeO^+ first adds to the π system of the reactant, then undergoes oxidative additions, and subsequently eliminates the products. On the other hand, in the reaction of toluene with FeO^+, the benzyl cation [16] is produced by either a hydride transfer (H_T^-) process or by a combination of $H_T^{\cdot}$ and electron transfer (*ET*). This archetypal reactivity scheme shows that FeO^+ (and its other first-row MO^+ relatives) promotes two fundamentally different types of reactions [1]: The first type involves a many-bond initiation step, such as *I* and *AE*, and the second type involves one-bond reactions, *e.g.* $H_T^{\cdot}$, or *ET*. Since FeO^+ exhibits a high-spin ground state ($^6\Sigma^+$), $H_T^{\cdot}$ and *ET* will conserve the total spin, while *I* and *AE* are not likely to do so; similarly, H_T^- and the $H_T^{\cdot}/ET$ combinations are by necessity not spin-conserving. Moreover, upon reductive elimination of the product from the insertion intermediate of an *I* process, *e.g.* water from the quartet ground state of $^4[H-Fe-OH]^+$, the minimal energy path continues to the $Fe^+(^6D)$ ground state and neutral water. Thus, the overall reaction $FeO^+(^6\Sigma^+) + H_2(^1\Sigma^+) \rightarrow Fe^+(^6D) + H_2O(^1A_1)$ is indeed spin-conserving. Therefore, at least two different spin states of FeO^+ can participate in the processes displayed in *Scheme 1*, and hence, more than one multiplicity may be involved in the reaction coordinate, such that it reflects TSR rather than SSR.

Electronic Structures of MO^+ Cations. – The origin of TSR can be traced back to the electronic structures of the MO^+ cations [1] [21], for which a qualitative molecular-orbital diagram is shown in *Fig. 1*. The valence orbitals can be subdivided[2]) into bonding (1σ, 2σ, 1π), nonbonding (1δ, 3σ), and antibonding (2π, 4σ) blocks. However, the 1δ, 2π, and 3σ orbitals are close enough in energy (within 1 eV) that they become quasi-degenerate and are subject to the interplay of orbital gap effects, *Hund*'s rule, and electron correlation.

In the MO^+ cations of the early transition metals, *e.g.* ScO^+, TiO^+, and VO^+, the bonding block (1σ, 2σ, 1π) will be filled first, and the remaining electrons will populate the nonbonding orbitals (1δ, 3σ), while the antibonding block is empty (2π, 4σ): Thus, the ground states of these cations can formally be represented by a triple bond, in analogy to the description of the carbon-monoxide molecule [21]. Accordingly, the bond dissociation energies (BDEs) of the MO^+ cations are quite high [23], such that, on thermodynamic grounds, the oxides of the early transition-metal are much less capable for C–H and C–C bond activation as compared to those of the late transition-metals onwards from MnO^+.

---

[1]) Although there is no reasonable doubt for the actual occurrence of the reaction $FeO^+ + H_2 \rightarrow Fe^+ + H_2O$ at thermal energy, the measured reaction efficiencies (defined as the ratio of the experimental rate constants to the gas-kinetic collision frequency) differ by almost an order of magnitude, depending on the method employed: Our FTICR measurements yielded an efficiency of *ca.* 0.01 [11a], while *Bohme* and coworkers reported a value of 0.006 [18] using a flowing afterglow technique, and *Armentrout* and coworkers obtained an efficiency of *ca.* 0.002 based on cross-section data [10a]. In collaboration with *Armentrout*'s and *Bohme*'s groups, we will try to resolve these discrepancies in the near future.

[2]) The transformation from configurations based on complex orbitals to those based on real orbitals (*Fig. 1*) was carried out by an expansion of the appropriate determinant expressions. Each angular momentum state, with the exception of $\Sigma^{\pm}$, gives rise to two species of different symmetries; for the expansion technique, see [22].

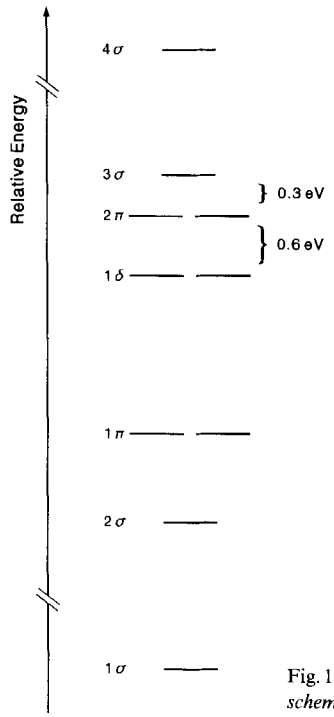

Fig. 1. *Qualitative molecular-orbital scheme for MO^+ cations*

With one additional electron, the ground state of CrO^+ is either the triply bonded $^4\Sigma^+$ or the $^4\Pi$ state which populates are 2π orbital instead of 3σ. Both states suffer from instabilities which considerably weaken the CrO^+ bond. Thus, $^4\Sigma^+$ must involve bonding between Cr^0 and O^+. Similarly, $^4\Pi$ involves the s^1d^4 excited state of Cr^+ in the bonding. CrO^+ occupies, therefore, an intermediate situation between the early and late transition-metal oxides.

In the series from MnO^+ to CuO^+, the bonding situation is more complex (*Table*). With respect to the quasi-degenerate 1δ, 2π, and 3σ orbitals, these binary metal-oxide cations possess ground states of high-spin multiplicities, while the first excited states are low-spin coupled. For MnO^+, the ground state is either $^5\Pi$ or $^5\Sigma^+$, depending on the level of calculation, and these two states only differ for the occupation of the 2π and 3σ orbitals. In any event, these two states represent a quasi-degenerate manifold. Noteworthy, MnO^+ also has a low-lying state of even higher multiplicity, *i.e.*, MnO^+ ($^7\Pi$), which derives from an excitation of one electron in $^5MnO^+$ from the bonding block into the non- or anti-bonding block (see below).

A first step in the conceptualization of the reactivity patterns of MO^+ cations is provided by the use of analogies from main-group chemistry. MnO^+ ($^5\Sigma^+$), and the ground states of FeO^+–CuO^+ involve the electronic configuration $1\sigma^2 2\sigma^2 1\pi_x^2 1\pi_y^2 2\pi_x^1 2\pi_y^1$. Since the 1σ orbital is mainly the 2s orbital of oxygen, these ground states possess one σ bond and two π-type and mutually perpendicular three-electron bonds, *i.e.*, $1\pi_x^2 2\pi_x^1$, and $1\pi_y^2 2\pi_y^1$. This bonding manifold has a close analogy with the $^3\Sigma_g^-$ high-spin ground state of triplet oxygen, O_2 ($^3\Sigma_g^+$) [1] [21].

Table. *Bond Lengths* r_{M-O} [Å] *and Excitation Energies* ΔE [eV] *of the Low-Lying States of the* MO^+ *Cations for* $M = Mn–Cu$ *as Obtained at the NLSD*[a]) *and CASPT2D*[b]) *Levels of Theory*[c])

	State[d])	Occupancy	r_{M-O} [Å]	ΔE [NLSD]	ΔE [CASPT2D]
MnO^+	$^5\Pi$	$1\sigma^2 2\sigma^2 1\pi^4 1\delta^2 2\pi^1 3\sigma^1$	1.59	0.0	0.1
	$^5\Sigma^+$	$1\sigma^2 2\sigma^2 1\pi^4 1\delta^2 2\pi^2 3\sigma^0$	1.58	0.1	0.0
	$^7\Pi$	$1\sigma^2 2\sigma^2 1\pi^3 1\delta^2 2\pi^2 3\sigma^1$	1.83	0.5	1.0
	$^3\Delta_1$	$1\sigma^2 2\sigma^2 1\pi^4 1\delta^3 2\pi^0 3\sigma^1$	1.51	1.5	3.0
	$^3\Delta_2/^3\Sigma^-$	$1\sigma^2 2\sigma^2 1\pi^4 1\delta^2 2\pi^2 3\sigma^0$	1.59	1.6	
FeO^+	$^6\Sigma^+$	$1\sigma^2 2\sigma^2 1\pi^4 1\delta^2 2\pi^2 3\sigma^1$	1.62	0.0	0.0
	$^4\Delta_1$	$1\sigma^2 2\sigma^2 1\pi^4 1\delta^3 2\pi^2 3\sigma^0$	1.56	1.0	
	$^4\Pi/^4\Phi$	$1\sigma^2 2\sigma^2 1\pi^4 1\delta^3 2\pi^1 3\sigma^1$	1.57	1.2	0.5[e])
	$^4\Gamma/^4\Delta_2$	$1\sigma^2 2\sigma^2 1\pi^4 1\delta^2 2\pi^2 3\sigma^1$	1.61	1.3	
	$^4\Delta_3/^4\Sigma^-$	$1\sigma^2 2\sigma^2 1\pi^4 1\delta^2 2\pi^2 3\sigma^1$	1.56	1.4	
CoO^+	$^5\Delta$	$1\sigma^2 2\sigma^2 1\pi^4 1\delta^3 2\pi^2 3\sigma^1$	1.63	0.0	
	$^3\Sigma^-$	$1\sigma^2 2\sigma^2 1\pi^4 1\delta^4 2\pi^2 3\sigma^0$	1.55	1.0	
	$^3\Pi$	$1\sigma^2 2\sigma^2 1\pi^4 1\delta^4 2\pi^1 3\sigma^1$	1.55	1.2	
	$^3\Delta/^3\Sigma^-$	$1\sigma^2 2\sigma^2 1\pi^4 1\delta^3 2\pi^2 3\sigma^1$	1.63	1.4	
NiO^+	$^4\Sigma^-$	$1\sigma^2 2\sigma^2 1\pi^4 1\delta^4 2\pi^2 3\sigma^1$	1.63	0.0	
	$^4\Delta$	$1\sigma^2 2\sigma^2 1\pi^4 1\delta^3 2\pi^2 1\sigma^2$	1.74	1.1	
	$^2\Delta/^2\Sigma^+$	$1\sigma^2 2\sigma^2 1\pi^4 1\delta^4 2\pi^2 3\sigma^1$	1.62	1.3	
	$^2\Pi$	$1\sigma^2 2\sigma^2 1\pi^4 1\delta^4 2\pi^1 3\sigma^2$	1.63	1.4	
CuO^+	$^3\Sigma^-$	$1\sigma^2 2\sigma^2 1\pi^4 1\delta^4 2\pi^2 3\sigma^2$	1.76	0.0	
	$^3\Pi$	$1\sigma^2 2\sigma^2 1\pi^4 1\delta^4 1\pi^3 3\sigma^1$	1.75	0.8	
	$^1\Delta/^1\Sigma^+$	$1\sigma^2 2\sigma^2 1\pi^4 1\delta^4 2\pi^2 3\sigma^2$	1.73	1.4	

[a]) NLSD stands for *non-local spin density* and refers to a density functional theory approach; for further details of our computation, see [1].

[b]) CASPT2D stands for *complete active space – 2nd order perturbation theory – using a diagonal zero-order Hamiltonian*; for details, see [1] [24].

[c]) Data taken from [1] [2] [19] [25].

[d]) In some cases, the computed real determinants transform to combinations of two complex configurations which are used to designate the term symbols; see [22].

[e]) Here, the CASPT2D approach separates the two states; $^4\Phi$ is at $\Delta E = 0.5$ eV [26].

The O_2 analogy carries over to the low-spin Δ-type excited states of MO^+ which possess the valence configuration $1\sigma^2 2\sigma^2 1\pi_x^2 1\pi_y^2 2\pi_x^2$ and $1\sigma^2 2\sigma^2 1\pi_x^2 1\pi_y^2 2\pi_y^2$, resembling the $^1\Delta_g$ state of dioxygen. Much as in singlet oxygen, the perfect-pairing low-spin Δ states of MO^+ suffer from four-electron repulsion in the filled π subshell (*Scheme 2, a*). To avoid the repulsion, all MO^+ cations trade off perfect-pairing with the more favorable high-spin situation (*Scheme 2, b*) that possesses a σ and two resonating three-electron π bonds [27], as the triplet ground state of dioxygen does. The $^5\Pi$ state of MnO^+ and its analogs, *i.e.*, FeO^+ ($^4\Phi$ and $^4\Pi$), CoO^+ ($^3\Pi$), and NiO^+ ($^2\Pi$), share the same valence shell ($1\sigma^2 2\sigma^2 1\pi_x^2 1\pi_y^2 2\pi_x^1$, or $1\sigma^2 2\sigma^2 1\pi_x^2 1\pi_y^2 2\pi_y^1$) and can be classified as π-type radicals in analogy to the $^2\Pi$ ground state of the $NO^{\cdot}$ radical (*Scheme 2, c*). All other low-lying excited states in the *Table*, *i.e.*, FeO^+ ($^4\Delta$ and $^4\Gamma$), CoO^+ ($^3\Sigma^-$), NiO^+ ($^4\Delta$), can be represented by the $^3O_2$-like σ–π valence character in *Scheme 2, b*.

Despite these similarities of the metal oxide cations, MnO^+ is an exception to some extent. At first, it has a quasi-degenerate $^5\Sigma^+/^5\Pi$ ground state, and secondly, it exhibits a low-lying state of even higher multiplicity, *i.e.*, MnO^+ ($^7\Pi$), while the $^3\Delta$ low-spin states are energetically more demanding (*Scheme 3*). This distinction of

Scheme 2

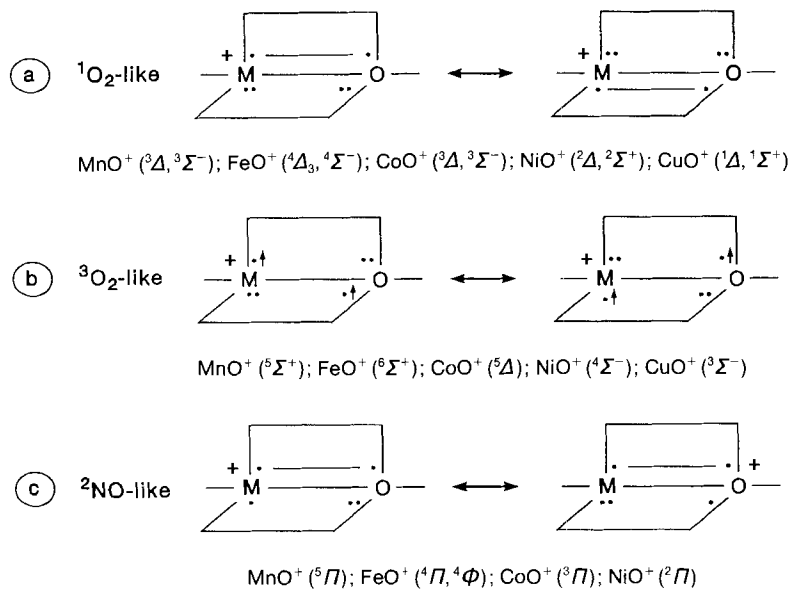

MnO^+ ($^3\Delta, ^3\Sigma^-$); FeO^+ ($^4\Delta_3, ^4\Sigma^-$); CoO^+ ($^3\Delta, ^3\Sigma^-$); NiO^+ ($^2\Delta, ^2\Sigma^+$); CuO^+ ($^1\Delta, ^1\Sigma^+$)

MnO^+ ($^5\Sigma^+$); FeO^+ ($^6\Sigma^+$); CoO^+ ($^5\Delta$); NiO^+ ($^4\Sigma^-$); CuO^+ ($^3\Sigma^-$)

MnO^+ ($^5\Pi$); FeO^+ ($^4\Pi, ^4\Phi$); CoO^+ ($^3\Pi$); NiO^+ ($^2\Pi$)

MnO^+ can be traced back to its electronic structure which exhibits a hole in the quasi-degenerate block, such that the $^5\Sigma^+$ and the $^5\Pi$ states also attain near degeneracy. Moreover, the corresponding $1\pi \rightarrow 2\pi$ (3σ) excitations to the $^7\Pi$ state of MnO^+ are not very demanding, since the energy difference between the 1π and 2π (3σ) orbitals is not too high, and it is compensated in part by exchange energy in the high-spin state. In contrast, the MO^+ cations of the other late transition metals are neither quasi-degenerate nor exhibit low-lying states of larger multiplicities, simply because of the number of electrons. For example, for FeO^+ the lowest possible excitation to an octuplet ($^8\Pi$) involves promotion from the 1π to the highly anti-bonding 4σ orbital (*Scheme 3*).

Scheme 3

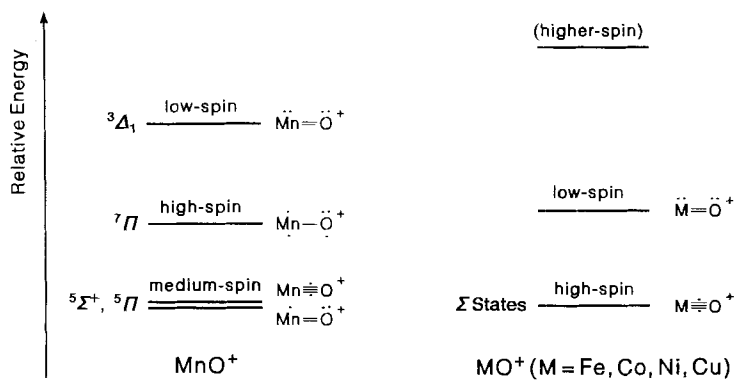

Principles of SSR and TSR in C–H Bond Activation. – As a case in point, we would like to analyze the role of TSR in the H–H and C–H bond activation by MO^+. The general mechanism [1] [10] involves an initial bond-activation phase (ⓐ) which is followed by an exit-phase (ⓑ) as depicted in *Eqn. 1* with no allusion to the spin situation.

$$MO^+ + R{-}H \xrightarrow{ⓐ} R{-}M^+{-}OH \text{ or } R^{\cdot}/MOH^+ \xrightarrow{ⓑ} M^+ + R{-}OH \qquad (1)$$

For all MO^+ cations considered here (M = Mn–Cu), *Reaction 1* is highly exothermic [2]. Therefore, the exit phase is located in the down-hill portion of the potential-energy hypersurface and, most likely, will not constitute a bottleneck. This conclusion is further supported by the magnitude of the intramolecular kinetic isotope effects associated with C–H bond activation of alkanes by MO^+ which range from $k_H/k_D = 2$–5, indicating that bond activation (ⓐ) is rate-determining [11b] [14b, c, e] [19]. In addition, our previous NLSD calculations [1] indicated rather low barriers in the exit channel (ⓑ) for the FeO^+/H_2 system.

The Principle of Spin Conservation. In a series of elegant studies, *Armentrout* has demonstrated that the reactivity of 'bare' transition-metal cations is highly dependent on the initial spin of the reactant [28]; for example, the excited ^4F state of Fe^+ was observed to react *ca.* 50 times faster with H_2 than the $Fe^+(^6D)$ ground state [29]. Thus, similar to main-group chemistry, spin conservation is important for reactions in organometallic chemistry as well.

From a more general point of view [30], the principle of spin-conservation determines the bonding capabilities, namely, *the maximum number of covalent bonds which can be formed for a given multiplicity*. There exist two ways in which a substrate can be activated under spin conservation. The first way involves the utilization of the unpaired electrons for single-bond abstractions (*e.g.* $H_T^{\cdot}$) or *ET*. For example, the $^3O_2$-like ground states of MO^+ are capable to abstract a H-atom from alkanes and form $R^{\cdot} + MOH^+$ which conserves the total spin. However, these processes are either only weakly exothermic or even endothermic for the metals under study, since they are associated with a net loss of resonance energy in the $^3O_2$-like ground states. Thus, atom abstraction is not very favorable much as O_2 ($^3\Sigma_g^-$) itself does not easily promote abstraction reactions with closed shell molecules [31]. *ET* Reactions could have been feasible for all MO^+ species; however, the ionization energies (*IE*s) of the neutral metal oxides are well below (< 9 eV [2b]) those of most organic substrates.

In general, it is more favorable to prepare *two* covalent bonds in the transition structures associated with R–H bond activations by MO^+ leading to inserted species of the type $[R{-}M{-}OH]^+$. Under the conditions of spin conservation, the $^3O_2$-like ground states of MO^+ can only achieve this bonding, when two electrons are unpaired and singlet-coupled with the triplet state of the reactant [6] [27] [32]. As an example, we refer to the VB crossing diagram for the formation of $R{-}Mn{-}OH^+$ from MnO^+ ($^5\Pi$) and R–H (singlet) (*Fig. 2*): In the VB scheme, avoided crossing of the $MnO^+ + R{-}H$ surface with the $^7\Pi$ state of MnO^+, and the triplet ^3RH allows for the formation of two new bonds while conserving spin; similar considerations apply for MnO^+ ($^5\Sigma^+$). Thus, R–H bond activation can proceed as SSR *via* avoided crossing with a 'prepared' excited state [32] which involves the MO^+ species in a higher spin situation relative to the ground state. While for MnO^+ the high-spin septet state is relatively low in energy, for FeO^+–CuO^+ this option does hardly exist, as it would require excitations into the antibonding 4σ orbitals.

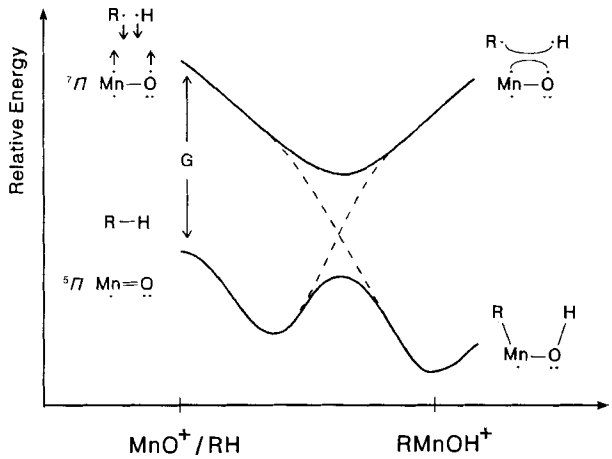

Fig. 2. *Schematic valence-bond crossing diagram for the ion/molecule reaction of a substrate R–H with* MnO^+ ($^5\Pi$) *to yield the insertion product* $^5[R–Mn–OH]^+$ via *crossing with the* MnO^+ ($^7\Pi$) + $^3[R–H]$ *surface*

As a consequence, the avoided crossing diagrams of these metal-oxide cations will involve larger promotion energy gaps (G) between the ground and the 'prepared' excited states, thus, a higher barrier, and also lead to less stable $[R–M–OH]^+$ species.

The Bond-Activation Phase. Recently [1], we have computed the relative energies of the reactant complex **1**, the inserted species **2**, and the associated TS **1/2** connecting them (*Fig. 3*). Indeed, on the sextet surface TS **1/2** ($^6A'$) ist 19 kcal/mol higher in energy as compared to the entrance channel of isolated FeO^+ ($^6\Sigma^+$) and H_2 ($^1\Sigma$), such that no

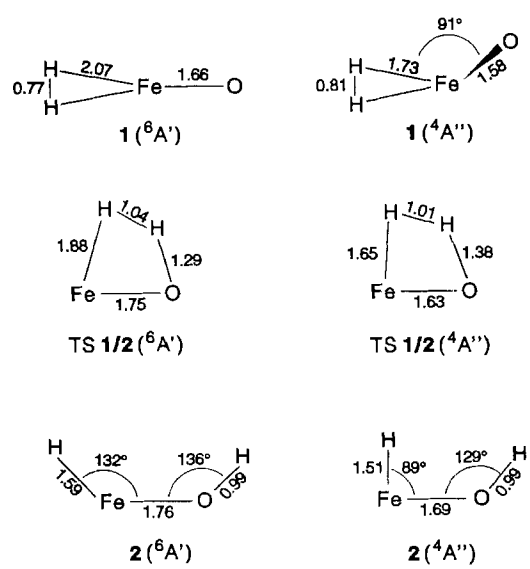

Fig. 3. *Calculated geometries* (bond lengths in Å and angles in degrees, NLSD level of theory) *of the sextet and quartet electromers in the reaction of* FeO^+ *with* H_2. Taken from [1].

reaction can occur *via* SSR at thermal energies. In fact, the relatively long bonds in the sextet TS and also in the insertion product **2** ($^6A'$) manifest the antibonding interactions imposed by the spin-conservation principle, since in the high-spin states two covalent bonds cannot be formed efficiently.

How can the late transition-metal oxide cations FeO^+–CuO^+ circumvent the unfavorable bond-activation phase on the high-spin surface? The answer to this question is latent in *Scheme 3* which shows that excitation to low-spin states requires only *ca.* 1 eV for these MO^+ cations. Since the low-spin states possess low-lying empty orbitals (*Table*), each of these has a closely spaced 'prepared' high-spin state. In analogy to the VB crossing diagram in *Fig. 2*, these will lead to energetically favorable low-spin TS and low-spin insertion products, which obey spin conservation. Let us illustrate this point for the $^4\Pi$, $^4\Phi$, and $^4\Delta$ states of FeO^+ which lie *ca.* 1 eV above the $^6\Sigma^+$ ground state. In the VB crossing scheme, these states have the $^6\Pi$, $^6\Phi$, and $^6\Delta$ 'prepared' excited states [32] which are obtained *via* $1\pi \rightarrow 2\pi$ promotions. These excitations will break the π bond of FeO^+ and provide the quartet states with two-bond capabilities while conserving spin when these interact with R–H. Thus, according to the VB scheme (*Fig. 2*), the low promotion energy gaps will result in low barriers for bond activation. Indeed, the computations reveal that TS **1/2** ($^4A''$) is 16 kcal/mol below the entrance channel of the quartet asymptote $^4FeO^+ + H_2$ and even only slightly above the ground state entrance channel FeO^+ ($^6\Sigma^+$) + H_2 ($^1\Sigma^+$)[3]). Moreover, the $^4A''$ state represents the ground state of the insertion product **2**. The more compact geometries of the low-spin structures as compared to the sextet species (*Fig. 3*) are in line with this description.

The situation outlined for the reaction of FeO^+ with H_2 is representative for the other MO^+/R–H combinations as well (M = Co, Ni, and Cu). As a result of this relationship between the low-spin and the high-spin surfaces, the bond-activation phases will be typified by the spin-state intersections and conform to TSR. These features are exempli-

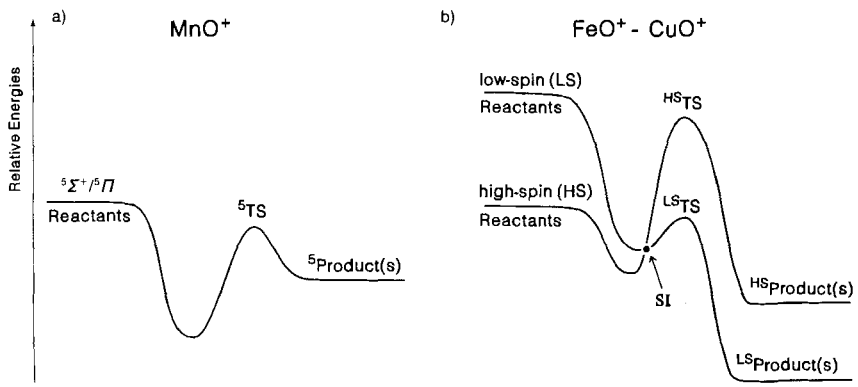

Fig. 4. *Qualitative features of single and two-state reactivity* (SSR and TSR) *in bond activations of R–H molecules by metal-oxide cations. a*) SSR in the reactions of MnO^+ ($^5\Sigma^+$ or $^5\Pi$). *b*) TSRs in the reactions for FeO^+–CuO^+.

[3]) Relative energies at the CASPT2D level of theory (isolated FeO^+ ($^6\Sigma^+$) + H_2 ($^1\Sigma^+$) = 0): **1** ($^6A'$) = −5 kcal/mol, **1** ($^4A''$) = 3 kcal/mol, TS **1/2** ($^6A'$) = 19 kcal/mol, TS **1/2** ($^4A''$) = 6 kcal/mol, **2** ($^6A'$) = −14 kcal/mol, **2** ($^4A''$) = −25 kcal/mol. For a complete discussion of the energetics as well as an error analysis, see [1].

fied in *Fig. 4* in which the SSR in the case of $^5MnO^+$ (*Fig. 4, a*) contrasts the need of TSRs for FeO^+–CuO^+ (*Fig. 4, b*).

Energetic Features of SSR. In the SSR picture, the reaction of MO^+ with R–H follows a classical point of view, and its efficiency will depend on the lifetimes (stabilities) of the reactant complexes, the heights of the barriers associated with the transition structures, and the stabilities of the insertion products on the corresponding single spin surfaces.

Primarily, these energetics will depend on the intrinsic thermodynamics of the reactants, *i.e.*, MO^+–O and R–H bond dissociation energies as well as the overall reaction exothermicities. According to *Fig. 2*, the heights of the barriers are related to the sizes of the promotion energy gaps between the reactants and the corresponding 'prepared' excited states and the singlet/triplet gaps of the R–H bonds. Hence, for a given MO^+ cation, the reaction will become more efficient, the smaller the triplet excitation of the R–H bond is [33]. A second important energetic factor is related with the charge-transfer stabilization in the TS, which arises from mixing of the charge-transfer configurations into the TS [34]. For example, the configuration $^5[MnO/R{-}H^+]$ which involves electron transfer from the σ_{R-H} orbital to either the 3σ orbital in MnO^+ ($^5\Sigma^+$) or to the 2π orbital in MnO^+ ($^5\Pi$) will mix with $^5[MnO^+/R{-}H]$ as well as the corresponding 'prepared' excited states (*Fig. 2*); all these effects will stabilize the TS. Thus, besides thermochemistry and lifetime effects [11] [19], two additional fundamental quantities affect the bond-activation phase in SSR, namely, the singlet/triplet gap of the R–H bond and the ionization energies of R–H and MO. This conclusion is in line with the experimental observation that the reactivity of MO^+ species increases when proceeding from H_2 to CH_4 and larger alkanes.

A case in point is the poor activating ability of CrO^+. Here, the low electron affinity [2b] render the process inefficient. Thus, CrO^+ is a poorer acceptor relative to all the late MO^+ species, and, consequently, the corresponding TS for insertion enjoys less stabilization due to charge-transfer mixing.

Features of TSR. Unlike the $MnO^+/R{-}H$ system, in the bond-activation phases of FeO^+–CuO^+, TSR must involve a barrier crossing *and* a spin-inversion junction along the reaction coordinate (*Fig. 4, b*). For example, in the reaction of FeO^+ ($^6\Sigma^+$) with H_2, the initially formed or vibrationally excited encounter complex **1** ($^6A'$) in *Fig. 3* has to invert spin and pass over to the barrier on the low-spin surface in order to achieve reactivity at room temperature[1]).

As far as the barrier heights on the low- and the high-spin surfaces are concerned, the previous discussion reveals that for the low-spin excited states of MO^+ (M = Fe–Cu) R–H bond activation will be more facile as compared to the high-spin surfaces. How does the barrier height depend on the nature of the metal? Let us make a simplifying and reasonable assumption that unpairing the π bond in MO^+ (*Fig. 2*) will require roughly the same amount of energies for FeO^+–CuO^+. Then, simply the number of electrons determines reactivity, and the more electrons MO^+ has, the more repulsive interactions with RH will arise, and as such the barrier heights will increase in going from Fe to Cu. This conclusion is indeed supported by the experimental observation that FeO^+ is much more effective in R–H bond activation as compared to CoO^+ and NiO^+. Moreover, since the spin-orbit coupling constants increase from Fe^+ to Cu^+ [35], the high reactivity of FeO^+ does indeed seem to reflect barrier height rather than spin-inversion probabilities. Thus, it is obvious that TSR is not described by the SI junction alone, but 'classical' parameters, such as barrier heights, are also essential.

The spin-inversion probability (P_{SI}) [36] between both surfaces is of fundamental importance for TSR. One important factor which influences P_{SI} is the spin-orbit coupling (SOC)[4]). In the $MO^+/R-H$ systems the metal-related SOC terms are significantly larger than those of the other atoms. Therefore, we can expect that the corresponding matrix elements $\langle H_{SO} \rangle$, which determine SOC, will depend on the degree of electron delocalization in the intermediates and will be fractions of the corresponding atomic constants of M^+ (see *e.g.* [37]). The latter quantities increase with nuclear charge from Fe^+ to Cu^+, *i.e.*, 416 cm^{-1}, 530 cm^{-1}, 663 cm^{-1}, and 828 cm^{-1}, respectively [36b]. As a very rough and zero-order approximation in order to assess to what extent the SI junctions exercise control over the bond-activation phases, we may use the *Landau-Zerner* formula (*Eqn. 2*) [38] for a semi-classical treatment of P_{SI} at the point of intersection of the high- and low-spin states [4] [25].

$$P_{SI} = 1 - \exp\{-4\pi^2 \langle H_{SO} \rangle^2 / [hv|F_{HS} - F_{LS}|]\} \quad (2)$$

Here, $\langle H_{SO} \rangle$ is the spin-orbit matrix element, v the velocity of the nuclei reaching the spin-inversion junction, and $|F_{HS} - F_{LS}|$ the absolute difference in the slopes of the corresponding curves near the crossing point. Thus, large P_{SI} require large SOC matrix elements, low velocities (lower temperatures), and small differences in the slopes of the intersecting curves. Indeed, preliminary calculations [39] of the reaction of FeO^+ with H_2 reveal SOC matrix elements between 28 and 235 cm^{-1} (*i.e.* ~ 7–50% of the Fe^+ atomic constant) for the $^6A'$ and $^4A''$ states of the reactant complex **1**, which leads to values of P_{SI} between 0.003 and 0.3.

As the matrix elements increase with the effective nuclear charge, P_{SI} is expected to rise from Fe to Cu. As we have argued before, FeO^+ is a more reactive bond activator than CoO^+ and NiO^+ which may reflect the favorable barrier of the low-spin surface for FeO^+. Thus, with regard to the experimentally measured efficiency of 0.001–0.01 for the reaction of FeO^+ with H_2, the calculated P_{SI} indicates that the SI junctions may contribute to the bottleneck in the bond-activation phases. However, the entire MO^+/H_2 series exhibits reactivity which is influenced by the interplay of P_{SI}, the barrier heights, and lifetime effects. Thus, the observation that NiO^+ is more reactive than CoO^+ may indeed be a manifestation of the SI bottleneck, while the FeO^+ reactivity is a manifestation of the preferred energetics. Within this context, it is intriguing that PtO^+ (formally isoelectronic to NiO^+) reacts quite efficiently with alkanes including methane [40] which is in line with the fact that the Pt^+ atomic constant is very large, such that the SI bottleneck vanishes.

The Exit Phase. For the completion of a hydroxylation process the inserted species $[R-M-OH]^+$ has to separate out into the products M^+ and R–OH *via* reductive elimination [1] [2] [10]. The TSR paradigm accounts for the observed reactivities of the high-spin ground states for FeO^+, CoO^+, and NiO^+ with R–H, in that bond activation involves the low-spin potential-energy surfaces. Accordingly, the products should also evolve as low-spin products, even if these do not correspond to the ground states, *e.g.* electronically excited $Fe^+(^4F)$ together with $H_2O(^1A_1)$ as opposed to $Fe^+(^6D)$ and H_2O which is the 6-kcal/mol more-stable exit channel. This means that the reaction $FeO^+ + H_2$ has an

[4]) However, in the present systems there exist additional perturbations which give rise to non-zero off-diagonal matrix elements, *i.e.*, rotational couplings [30b] [36]. Therefore, the *Born-Oppenheimer* approximation, *i.e.*, the separation of nuclear and electronic motions, is no longer an adequate description.

additional SI junction in the exit phase for Fe^+, while Co^+–Cu^+ which possess low-spin ground states [1] [41b] do not have this additional SI junction. Notwithstanding, MnO^+ and FeO^+ are the most reactive MO^+ cations which further supports the notion expressed in the outset that the bond-activation phase is rate-determining while the spin constraints of the exit phase are not efficiency-rate-determining.

The MnO^+/R–H systems do not dispose entirely of the spin-inversion dilemma, they simply postpone it to the exit channel (*Eqn. 3*), where the septuplet ground state of Mn^+ necessitates spin-inversion. An alternative without a necessity for any change in multiplicity involves formation of excited $^5Mn^+$ cations (*Eqn. 4*).

$$R{-}Mn^+{-}OH(^5A') \rightarrow Mn^+ (^7S) + R{-}OH (^1S) \quad (3)$$

$$R{-}Mn^+{-}OH(^5A') \rightarrow Mn^+ (^5S \text{ or } ^5D) + R{-}OH (^1S) \quad (4)$$

Since the excited states of Mn^+ cation (^5S, ^5D) lie 27 and 42 kcal/mol above the ^7S ground state, the spin-conserving channel (*Eqn. 4*) will be accessible only for those systems where hydroxylation is at least 27 kcal/mol exothermic with respect to ground state products (*Eqn. 3*). This reasoning explains the experimental finding [19] that for the MnO^+/H_2 system ($\Delta H_R = -50$ kcal/mol), besides hydrogen abstraction leading to $MnOH^+$, significant amounts of Mn^+ cation are formed. In contrast, for the MnO^+/CH_4 couple ($\Delta H_R = -22$ kcal/mol) the $H^{\cdot}_T$ channel predominates, while formation of Mn^+ is hardly observed, since the latter cannot proceed with spin-conservation (*Eqn. 3*).

The Radical Behavior of MnO^+. Until now, we have regarded the bond-activation phase as a two-bond process leading to $^5[R{-}Mn{-}OH]^+$. Nevertheless, the major product, which is observed in the ion/molecule reactions of MnO^+ with H_2 and CH_4, is $MnOH^+$ and the corresponding radicals [19], and $MnOH^+$ formation is also significant in the reactions of larger alkanes. This experimental finding implies that the bond-activation phase follows *Eqn. 5*:

$$MnO^+ + R{-}H \rightarrow MnOH^+ + R^{\cdot} \qquad \Delta H_R = -10 \text{ to } -20 \text{ kcal/mol} \quad (5)$$

However, since $MnOH^+$ cation exhibits a $^6A'$ ground state [19], and the radical $R^{\cdot}$ is necessarily a doublet, *Reaction 5* is spin-conserving and may simply be represented as the bond dissociation of the insertion product (*Eqn. 6*).

$$R{-}Mn^+{-}OH\ (^5A') \rightarrow MnOH^+\ (^6A') + R^{\cdot}\ (^2A') \quad (6)$$

Since the overall reactions (*Eqn. 5*) are exothermic, and there exists no spin restriction, $MnOH^+$ can simply arise from dissociation of rovibrationally excited $R{-}Mn^+{-}OH$. As a consequence, in the gas phase MnO^+ cation reacts with hydrocarbons predominantly by $H^{\cdot}_T$ and may, therefore, also be described as an oxygen-centered radical (right-hand resonance structures in *Scheme 2*, *b* and *c*).

SSR Options for $MO^+/R{-}H$ (M = Fe, CO, Ni). A conceivable way to bypass the SI bottleneck is by means of a one-bond activation, directly to a pair of radicals, *e.g.* $[R^{\cdot}/MOH^+]$. For example, $FeO^+(^6\Sigma^+)$ can abstract a hydrogen atom from the substrate to yield $FeOH^+(^5A'')$ and $R^{\cdot}(^2A)$. Thus, although the insertion product exhibits a low-spin ground state, *e.g.* **2** ($^4A''$), the radical pair may collapse to the high-spin addition product and proceeds directly to the product complex $R{-}OH/Fe^+$, as exemplified in *Fig. 5* by the guiding arrows in the potential-energy hypersurface. This option suffers from the en-

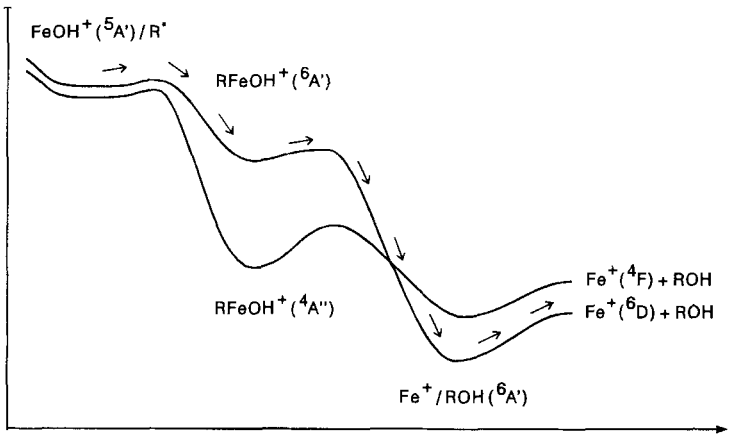

Fig. 5. *Competition of SSR and TSR in the reactions of FeO^+ with an R–H molecule.* The arrows illustrate how the radical pair may bypass the spin-inversion bottleneck on the high-spin surface.

ergetic disadvantage in comparison with the two-bond route, such that, energetically, there exists a strong bias for the TSR pathway. However, in situations where that R–H bond is weak, and the complexation energy of the reactant to the metal oxide cation is large [1] [2], the high-spin pathway may become energetically accessible. If so, a one-bond SSR pathway may effectively compete with TSR, especially since the SI bottleneck limits the efficiency of the latter mechanism.

Conclusions. – This article describes the features of TSR as compared to the classical SSR model in the bond activation of R–H by 'bare' MO^+ cations. It is shown that the superior reactivity of MnO^+ is related to the SSR mode of its bond-activation phase. The lower efficiencies in the reactions of FeO^+, CoO^+, and NiO^+ derive in part from TSR in the bond-activation phases of these MO^+ cations. In general, SSR deals with a uniform spin surface on which reactivity is dominated by energetic factors as the height of the barrier and the reaction exothermicity. While these factors do also play a role in TSR, the latter involves in addition the probability factors for the crossover of the spin-inversion junction from one multiplicity to another. Although we only address the MO^+/R–H systems in this article, there exists independent evidence [41] for the fact that spin inversion seems to be quite a common [28], though not general, route in gas-phase organometallic chemistry.

In the future, systematic studies of trends along and down the periodic table are indicated in order to discern rules of the barrier/multiplicity interplay in TSR. Furthermore, probing spin interconversion by selective population of spin sublevels [42] together with detailed theoretical treatments [43] will be required for a deeper understanding of spin-orbit coupling in polyatomic molecules. Notwithstanding these uncertainties, two-state reactivity appears to be a new paradigm in organometallic chemistry which offers wide perspectives, as it may help to describe seemingly different topics from ligand effects which tune reactivity in the gas phase, *e.g.* 'bare' *vs.* complexed FeO^+ [44] or FeX^+ cations bearing different covalently linked ligands X [45], all the way down to applied catalytic oxidations or to biochemistry, *e.g.* P-450 [13a].

This research has been sponsored by a grant of the *Volkswagen Stiftung*; the continuous support provided by the *Deutsche Forschungsgemeinschaft* and the *Fonds der Chemischen Industrie* to *H. S.* is acknowledged.

REFERENCES

[1] A. Fiedler, D. Schröder, S. Shaik, H. Schwarz, *J. Am. Chem. Soc.* **1994,** *116,* 10734.
[2] a) H. Schwarz, D. Schröder, Proceedings of the Robert A. Welch Foundation 38th Conference on Chemical Research, The Robert A. Welch Foundation, Houston, 1995, p. 287; b) D. Schröder, H. Schwarz, *Angew. Chem.*, in press; c) R. Zahradnik, *J. Mol. Catal.* **1993,** *82,* 865.
[3] a) R. A. More O'Ferrall, *J. Chem. Soc. B* **1970,** 274; b) W. P. Jencks, *Chem. Rev.* **1985,** *85,* 511; c) I. H. Williams, *Chem. Soc. Rev.* **1993,** *22,* 277.
[4] K. Fukui, 'Theory of Orientation and Stereoselection', Wiley-Interscience, New York, 1976.
[5] R. B. Woodward, R. Hoffmann, 'The Conservation of Orbital Symmetry', Academic Press, New York, 1970.
[6] A. Pross, S. S. Shaik, *Acc. Chem. Res.* **1983,** *16,* 363.
[7] R. Hoffmann, *Angew. Chem. Int. Ed.* **1982,** *21,* 711.
[8] a) M. L. Steigerwald, W. A. Goddard, III, *J. Am. Chem. Soc.* **1984,** *106,* 308; b) G. Ohanessian, W. A. Goddard, III, *Acc. Chem. Res.* **1990,** *23,* 386; c) E. A. Carter, W. A. Goddard, III, *J. Phys. Chem.* **1988,** *92,* 5679.
[9] N. Koga, K. Morokuma, *Chem. Rev.* **1991,** *91,* 823.
[10] a) D. E. Clemmer, Y.-M. Chen, F. A. Khan, P. B. Armentrout, *J. Phys. Chem.* **1994,** *98,* 6522; b) Y.-M. Chen, D. E. Clemmer, P. B. Armentrout, *J. Am. Chem. Soc.* **1994,** *116,* 7815.
[11] a) D. Schröder, A. Fiedler, M. F. Ryan, H. Schwarz, *J. Phys. Chem.* **1994,** *98,* 68; b) M. F. Ryan, A. Fiedler, D. Schröder, H. Schwarz, *Organometallics* **1994,** *13,* 4072.
[12] a) C. L. Hill, 'Activation and Functionalization of Alkanes', Wiley-Interscience, New York, 1989; b) J. A. Davies, P. L. Watson, J. F. Liebman, A. Greenberg, Eds., 'Selective Hydrocarbon Activation', VCH Publishers, Weinheim, 1990; c) D. H. R. Barton, A. E. Martell, D. T. Sawyer, Eds., 'The Activation of Dioxygen and Homogeneous Catalytic Oxidation', Plenum Press, New York, 1993.
[13] For example: a) P. R. Ortiz de Montellano, Ed., 'Cytochrome P-450: Structure, Mechanism and Biochemistry', Plenum Press, New York, 1986; b) L. I. Simándi, 'Dioxygen Activation and Homogeneous Catalytic Oxidation', Elsevier, Amsterdam, 1991; c) D. H. R. Barton, *Chem. Eng. News* **1995,** April 3, p. 28.
[14] a) T. C. Jackson, T. J. Carlin, B. S. Freiser, *J. Am. Chem. Soc.* **1986,** *108,* 1120; b) D. Schröder, H. Schwarz, *Angew. Chem. Int. Ed.* **1990,** *29,* 1431; c) D. Schröder, H. Schwarz, *ibid.* **1990,** *29,* 1433; D. Schröder, K. Eller, H. Schwarz, *Helv. Chim. Acta* **1990,** *73,* 380; e) D. Schröder, A. Fiedler, J. Hrušák, H. Schwarz, *J. Am. Chem. Soc.* **1992,** *114,* 1215.
[15] a) D. Schröder, H. Schwarz, *Helv. Chim. Acta* **1992,** *75,* 1281; b) M. F. Ryan, D. Stöckigt, H. Schwarz, *J. Am. Chem. Soc.* **1994,** *116,* 9565.
[16] D. Schröder, H. Florencio, W. Zummack, H. Schwarz, *Helv. Chim. Acta* **1992,** *75,* 1792.
[17] a) D. Schröder, J. Hrušák, H. Schwarz, *Helv. Chim. Acta* **1992,** *75,* 2215; b) H. Becker, D. Schröder, W. Zummack, H. Schwarz, *J. Am. Chem. Soc.* **1994,** *116,* 1096.
[18] V. Baranov, G. Javahery, A. C. Hopkinson, D. K. Bohme, submitted to *J. Am. Chem. Soc.*
[19] M. F. Ryan, A. Fiedler, D. Schröder, H. Schwarz, *J. Am. Chem. Soc.* **1995,** *117,* 2033.
[20] a) S. W. Buckner, J. R. Gord, B. S. Freiser, *J. Am. Chem. Soc.* **1988,** *110,* 6606; b) D. Stöckigt, Diploma Thesis, TU Berlin, 1991; c) Ref. 14b.
[21] E. A. Carter, W. A. Goddard, III, *J. Phys. Chem.* **1988,** *92,* 2109.
[22] P. C. Hiberty, C. Leforestier, *J. Am. Chem. Soc.* **1978,** *100,* 2012.
[23] E. R. Fisher, J. L. Elkind, D. E. Clemmer, R. Georgiadis, S. K. Loh, N. Aristov, L. S. Sunderlin, P. B. Armentrout, *J. Chem. Phys.* **1990,** *93,* 2676.
[24] K. Andersson, P.-Å. Malmqvist, B. O. Roos, A. J. Sadlej, K. Wolinski, *J. Phys. Chem.* **1990,** *94,* 5483.
[25] a) S. A. Mitchell, in 'Gas-Phase metal Reactions', Ed. A. Fontijn, Elsevier, Amsterdam, 1992, p. 249; b) Also see: P. E. M. Siegbahn, M. R. A. Blomberg, *Organometallics* **1994,** *13,* 354.
[26] A. Fiedler, J. Hrušák, W. Koch, H. Schwarz, *Chem. Phys. Lett.* **1993,** *211,* 242.
[27] S. S. Shaik, 'A Qualitative Valence Bond Model for Organic Reactions', in 'New Theoretical Concepts for Understanding Organic Reactions, J. Bertram', Ed. G. I. Csizinadia, NATO ASI Series, Vol. C267, Kluwer Publishers, Dordrecht, 1989, p. 165.
[28] P. B. Armentrout, *Science* **1991,** *251,* 175.

[29] J. L. Elkind, P. B. Armentrout, *J. Phys. Chem.* **1986,** *90,* 5736.
[30] a) E. Wigner, E. E. Witmer, *Z. Phys.* **1928,** *51,* 859; b) G. Herzberg, 'Molecular Spectra and Molecular Structure', 2nd edn., Van Nostrand Reinhold, New York, 1950, Vol. I, p. 315; c) C. Heinemann, J. Schwarz, W. Koch, H. Schwarz, *J. Chem. Phys.*, in press.
[31] E. G. Janzen, *Chem. Eng. News* **1994,** March 14, p. 4.
[32] a) S. S. Shaik, *J. Am. Chem. Soc.* **1981,** *103,* 3692; b) S. Shaik, *J. Mol. Liq.* **1994,** *61,* 49.
[33] a) S. S. Shaik, E. Canadell, *J. Am. Chem. Soc.* **1990,** *112,* 1446; b) S. S. Shaik, P. C. Hiberty, G. Ohanessian, J. M. Lefour, *J. Phys. Chem.* **1988,** *92,* 5086; c) A. Pross, H. Yamataka, S. Nagase, *J. Phys. Org. Chem.* **1991,** *4,* 135.
[34] M. W. Wong, A. Pross, L. Radom, *Isr. J. Chem.* **1993,** *33,* 415.
[35] I. V. Khudayakov, Y. A. Serebrennikov, N. J. Turro, *Chem. Rev.* **1993,** *93,* 537.
[36] a) S. P. McGlynn, T. Azumi, M. Kinoshita, 'The Triplet State', Prentice-Hall, Englewood Cliffs, 1969; b) H. Lefebvre-Brion, R. W. Field, 'Perturbations in the Spectra of Diatomic Molecules', Academic Press, New York, 1986; c) S. S. Shaik, *J. Am. Chem. Soc.* **1979,** *101,* 3184.
[37] D. Hippe, S. D. Peyerimhoff, *J. Chem. Phys.* **1992,** *96,* 3503.
[38] a) C. Zener, *Proc. R. Soc. London [Ser.] A* **1932,** *137,* 595; *ibid.* **1933,** *140,* 660; b) See also: W. Kauzmann, 'Quantum Chemistry', Academic Press, New York, 1957, p. 539.
[39] D. Danovich, S. Shaik, unpublished.
[40] a) R. Wesendrup, D. Schröder, H. Schwarz, *Angew. Chem Int. Ed.* **1994,** *33,* 1174; b) C. Heinemann, R. Wesendrup, H. Schwarz, *Chem. Phys. Lett.* **1995,** *239,* 75; c) C. Heinemann, W. Koch, H. Schwarz, submitted to *Chem. Phys. Lett.*
[41] a) R. H. Schultz, J. L. Elkind, P. B. Armentrout, *J. Am. Chem. Soc.* **1988,** *110,* 411; b) E. R. Fisher, R. H. Schultz, P. B. Armentrout, *J. Phys. Chem.* **1989,** *93,* 7382; c) S. D. Hanton, R. J. Noll, J. C. Weishaar, *ibid.* **1990,** *94,* 5655; d) C. Heinemann, N. Goldberg, I. C. Tornieporth-Oetting, T. M. Klapötke, H. Schwarz, *Angew. Chem. Int. Ed.* **1995,** *34,* 213; e) H. H. Cornehl, C. Heinemann, D. Schröder, H. Schwarz, *Organometallics* **1995,** *14,* 992; f) M. C. Holthausen, A. Fiedler, H. Schwarz, W. Koch, *Angew. Chem.*, in press.
[42] a) M. A. El-Sayed, *Annu. Rev. Phys. Chem.* **1975,** *26,* 235; b) B. Dillinger, R. M. Hochstrasser, A. B. Smith, III, *J. Am. Chem. Soc.* **1977,** *99,* 5834.
[43] For example: C. M. Marian, *Ber. Bunsenges. Phys. Chem.* **1995,** *99,* 254.
[44] D. Stöckigt, H. Schwarz, *Chem. Ber.* **1994,** *127,* 2499.
[45] D. Schröder, J. Hrušák, H. Schwarz, *Ber. Bunsenges. Phys. Chem.* **1993,** *97,* 1085.